Am J Cancer Res 2020;10(9):2909-2918
www.ajcr.us /ISSN:2156-6976/ajcr0117947

Original Article

TRIP13 predicts poor prognosis in clear cell renal cell carcinoma

Adam Kowalewski[1], Damian Jaworski[1], Paulina Antosik[1], Marta Smolińska[1], Joanna Ligmanowska[1], Dariusz Grzanka[1], Łukasz Szylberg[1,2]

[1]Department of Clinical Pathomorphology, Collegium Medicum in Bydgoszcz, Nicolaus Copernicus University in Torun, Poland; [2]Department of Tumor Pathology and Pathomorphology, Oncology Centre-Prof. Franciszek Łukaszczyk Memorial Hospital, Bydgoszcz, Poland

Received July 10, 2020; Accepted August 3, 2020; Epub September 1, 2020; Published September 15, 2020

Abstract: What is the leading molecular mechanism that causes broad resistance to systemic therapies remains a key question in renal cancer related research. We explored associations of TRIP13 expression with the clinical course using the tissue microarray (TMA). The TMA contained specimens from 87 patients diagnosed with clear cell renal cell carcinoma (ccRCC). We performed immunohistochemistry to investigate TRIP13 protein expression levels. The overall survival (OS) was analyzed using the Kaplan-Meier method and log-rank statistics. Univariate and multivariate analyses were conducted using Cox proportional hazard models. Median follow up for the TMA cohort was 7.0 years. Tissues from 28.74% of patients demonstrated high TRIP13 expression. Mean TRIP13 expression in TRIP13-rich tumors was significantly higher comparing to adjacent normal tissues ($P < 0.05$). TRIP13 expression did not significantly correlate with stage nor tumor grade ($P > 0.05$). Elevated expression of TRIP13 served as an independent unfavorable prognostic indicator of survival in ccRCC ($P < 0.05$). TRIP13 overexpression predicts poor prognosis in ccRCC. Together with the emerging reports, this observation raises a suspicion that TRIP13 is a substantial driver of resistance to systemic therapies against kidney cancer.

Keywords: TRIP13, ccRCC, kidney cancer, renal carcinoma, expression, prognosis, survival, OS

Introduction

Renal cell carcinoma (RCC) is among the 10 most common cancers in both men and women, and its incidence is on the rise. In 2020, 73,750 new cases and 14,830 deaths due to RCC will occur in the US and over 400,000 new cases will occur worldwide [1]. Up to 30-40% of RCC cases are present as metastatic disease, either initially or after curative treatment [2]. The most common subtype, clear cell renal cell carcinoma (ccRCC), arises from the proximal convoluted tubule cells and accounts for approximately 70% of all cases [3]. Despite significant improvements in the clinical management over the last decade, most patients with metastatic ccRCC succumb to cancer progression within 1.5 years [4].

The exceptional intratumoral heterogeneity of RCC represents a considerable challenge limiting the efficacy of established systemic therapies [5]. Such treatment often further exacerbates the heterogeneity and leads to outgrowth of tumor cell subclones with resistance properties, including the resistance to apoptosis [6, 7]. The accumulating alterations found in both intrinsic and extrinsic apoptotic pathways aberrantly extend cells viability and eventually contribute to cancer progression [8]. Since apoptosis causes negligible damage to adjacent tissues [9], the apoptotic pathway-targeted therapies emerge as particularly promising strategy for RCC treatment.

TRIP13 is a protein encoded by *TRIP13* gene. Recent evidence implicates TRIP13 in various cell cycle phases, including meiosis, G2/Prophase and during the mitotic spindle assembly checkpoint (SAC) activation. TRIP13 is required for the development of higher-order chromosome structures and contributes to synaptonemal complex formation. It also promotes early steps of the DNA double-strand breaks (DSBs)

repair process. The latest reports together with in silico analysis, indicate its prominent role in driving tumorigenesis.

The Human Pathology Atlas is based on a systems-based analysis of the transcriptome of 17 main cancer types using data from 8,000 patients [10]. A national supercomputer center was used to analyze more than 2.5 petabytes of underlying publicly available data from the Cancer Genome Atlas (TCGA) to generate 900,000 survival plots describing the consequence of RNA and protein levels on clinical survival. All the data in the knowledge resource allows exploration of the human proteome. In this study, we explore the clinical association of TRIP13 with ccRCC histology and oncologic outcomes using the tissue microarray (TMA) ccRCC cohort, and validate these findings in TCGA.

Materials and methods

Tissue microarray

Tissue microarray (TMA) slide was obtained from a commercial supplier (US Biomax, Rockville, MD; TMA catalog number HKid-CRC180-Sur-01). The TMA (HKid-CRC180Sur-01) contained specimens from 92 patients, tumor and matched normal adjacent tissue (1 core/case), followed up for 7 years. Cores derived from 3 patients were missing, therefore these patients were excluded from the analysis. Retrievable patient data included age, pathology diagnosis, TNM, grade, stage and overall survival. The quality of the TMA was additionally approved by our pathologist. The study follows the principles of the Declaration of Helsinki. The tissues were collected under the highest ethical standards and HIPPA approved protocols with the donor being informed completely and with their consent. Since the tissues were commercially purchased, the study has been exempted from requiring ethical approval.

Immunohistochemistry

The TMA slide was processed at the Department of Clinical Pathology. The primary rabbit polyclonal anti-TRIP13 (HPA005727) antibody (Sigma-Aldrich, Merck KGaA, Darmstadt, Germany) was applied to estimate the expression of TRIP13 protein. The protocol has been standardized using a series of positive and negative control reactions. The positive control reaction was performed on a tissue model selected according to reference sources (The Human Protein Atlas: http://www.proteinatlas.org) and the antibody data-sheet. TRIP13 positive control reaction was performed on pancreatic cancer tissue showing cytoplasmic and nuclear expression. All negative control reactions were performed on additionally analyzed tissue sections, by substituting the primary antibody with a solution of 1% BSA (bovine serum albumin) diluted in PBS (phosphate buffered saline). Immunohistochemical staining was performed using primary rabbit polyclonal anti-TRIP13 (1:200) antibody and visualization system EnVisionFlex+ Anti-Mouse/Rabbit HRP-Labeled Polymer (Dako, Agilent Technologies) on an Autostainer Link48 platform. Finally, tissue sections were dehydrated in ethanol of increasing concentration (from 80% to 98%), then cleared in a series of xylenes (from I to IV) and coverslipped in a medium (Dako, Agilent Technologies, USA).

IHC analysis and scoring

Initially, two experienced pathologists blinded to the clinical data evaluated the immunostained slides using the light microscope ELIPSE E800 (Nikon Instruments Europe, Amsterdam, Netherlands) at 20× and 40× original objective magnification. IHC revealed cytoplasmic and nuclear TRIP13 expression.

The cytoplasmic staining intensity of cells and percentage of cells at each staining intensity level were determined for each fixed core in the TMA. Staining intensity was graded as 0 (negative), 1+ (weak), 2+ (modarate), and 3+ (strong). The H-score was assigned using the following formula: [1 × (% cells 1+) + 2 × (% cells 2+) + 3 × (% cells 3+)], obtaining a value from 0 to 300.

The nuclear expression evaluation was scored on a two-point scale: 0 (negative IHC reaction result) and 1 (positive IHC reaction result).

Statistical analysis

All the statistical analyses were performed using Statistica version 10 (StatSoft) and Microsoft Excel 2019. The comparative studies were analyzed statistically using the nonparametric chi-square test. The p value < 0.05 was considered statistically significant.

Table 1. Baseline characteristics of TMA (n = 87) patient cohort

Clinical information	*n* (%)
Age, yr	
Mean	59.0
Range	29-83
Stage	
I	58 (66.67)
II	17 (19.54)
III	3 (3.45)
IV	2 (2.30)
Unknown	0 (0.00)
T Stage	
T1	62 (71.26)
T2	17 (19.54)
T3	4 (4.60)
Unknown	4 (4.60)
Lymph nodes	
N1	1 (1.15)
N0/Nx	84 (96.55)
Unknown	2 (2.30)
Metastasis	
Yes	2 (2.30)
No	85 (97.70)
Grade	
G1	32 (36.78)
G1-G2	14 (16.09)
G2	27 (31.03)
G2-G3	4 (4.60)
G3	9 (10.34)
G3-G4	1 (1.15)
Median follow up time	7.0
Disease course	
Alive	59 (67.82)
Dead	28 (32.18)

Results

The location and expression of TRIP13 protein in ccRCC TMA cohort

IHC was performed on 87 pairs of ccRCC and corresponding normal tissues. Five cores of corresponding tissues were lost during IHC staining procedure. **Table 1** summarizes the characteristics of the TMA cohort. The mean age of patients was 59 years (range: 29-83 years) and the median follow-up was 7.0 years.

Cytoplasmic TRIP13 staining was observed in 77 (88.51%) of 87 ccRCC tissues and the median expression was 100 (interquartile range 0-215). Among adjacent controls, 70 (85.37%) of 82 cores were positive and the median expression was 115 (interquartile range 70-200). Cytoplasmic expressions of TRIP13 in ccRCC tissues were lower than those in adjacent controls ($P < 0.05$, **Figure 1A**). Next, we dichotomized the cytoplasmic expressions of TRIP13 to low expression and high expression. Using the tool *Cutoff Finder,* we set the best cutoff at 105 [11]. Mean TRIP13 expression in TRIP13-rich tumors was significantly higher comparing to adjacent normal tissues ($P < 0.05$, **Figure 1B**). Similarly, adjacent normal tissues were characterized by elevated TRIP13 expression when compared to TRIP13-depleted tumors ($P < 0.05$) (**Figure 1C**).

Nuclear TRIP13 staining was observed in 14 cancer tissues (16.28%) (**Figure 2A**) and only in 2 adjacent normal tissues (2.44%) (**Figure 2B**). This difference was statistically significant ($P < 0.05$).

Clinical course and TRIP13 protein expression in ccRCC TMA cohort

TRIP13 protein expression did not significantly correlate with TNM stage nor tumor grade (both $P > 0.05$). Univariate analysis revealed that patients with high cytoplasmic TRIP13 protein expression had significantly shorter OS comparing to those with low expression ($P < 0.05$, HR = 2.88 [1.35-6.15]) (**Figure 3**). We found no significant association between the presence of TRIP13 nuclear expression and OS (**Figure 4**). In conclusion, TRIP13 overexpression predicts poor prognosis in ccRCC. Together with the emerging reports, this observation raises a suspicion that TRIP13 is a substantial driver of resistance to systemic therapies against kidney cancer.

Discussion

TCGA ccRCC cohort analysis

We found that cytoplasmic TRIP13 protein overexpression significantly correlates with poor survival in ccRCC patients. To evaluate whether the expression of TRIP13 mRNA was also associated with the clinical course of the disease, we accessed TCGA database. All transcriptomics information were obtained employing the Human Pathology Atlas, the separate part of The Human Protein Atlas available from www.

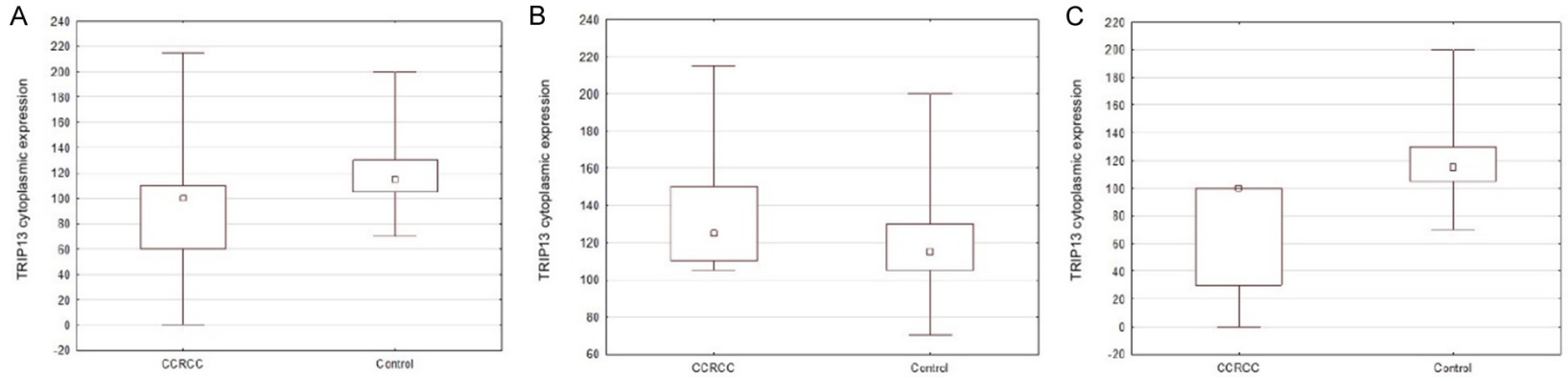

Figure 1. A. Cytoplasmic expression of TRIP13 in Clear Cell Renal Cell Carcinoma (CCRCC) and adjacent normal tissue (Control). B. Cytoplasmic TRIP13 expression in TRIP13-rich CCRCC and control. C. Cytoplasmic TRIP13 expression in TRIP13-depleted CCRCC and control.

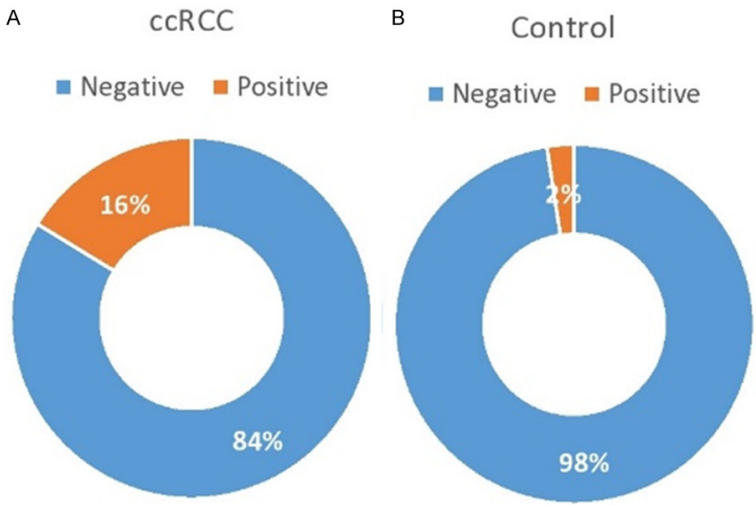

Figure 2. Prevalence of positive TRIP13 nuclear expression among (A) clear cell Renal Cell Carcinoma tissues, and (B) adjacent normal tissues (Control).

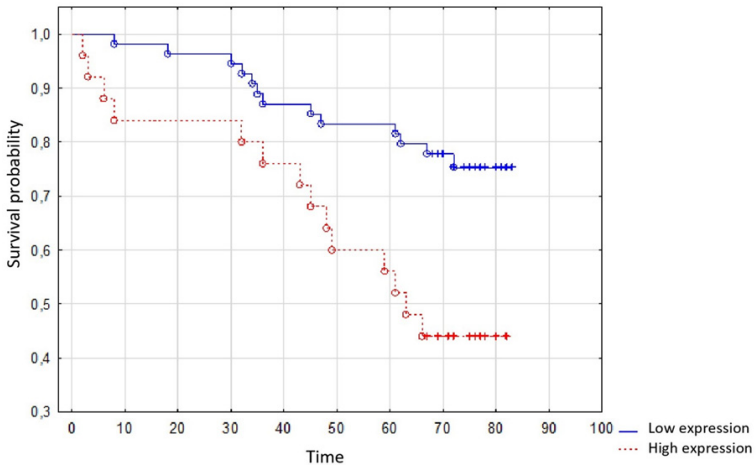

Figure 3. The survival curve of clear cell Renal Cell Carcinoma patients according to TRIP13 cytoplasmic expression.

proteinatlas.org. TCGA cohort consisted of 528 patients diagnosed with ccRCC [12]. The available characteristics of study subjects are summarized in **Table 2**. The mean age of patients was 60.5 years (range: 26-90 years) and the median follow-up was 3.28 years. The TCGA RNA-seq data was mapped using the Ensembl gene id available from TCGA, and the FPKMs (number Fragments Per Kilobase of exon per Million reads) for *TRIP13* were subsequently used for quantification of expression with a detection threshold of 1 FPKM. Based on the FPKM value of *TRIP13*, patients were classified into two expression groups. To choose the best FPKM cutoff for grouping the patients most significantly, all FPKM values from the 20th to 80th percentiles were used to group the patients, significant differences in the survival outcomes of the groups were examined and the value yielding the lowest log-rank *P* value (3.4e-11) was selected. 109 of 528 (20.64%) patients had higher expression than the established cutoff. The prognosis of each group of patients was examined by Kaplan-Meier survival estimators and the survival outcomes of the two groups were compared by log-rank tests. The five-year survival was reached by 70% of patients with low *TRIP13* expression and 39% of those with high expression. Taken together, TRIP13 mRNA expression is prognostic and its high expression is unfavourable in RCC ($P < 0.05$), according to TCGA.

The Human Protein Atlas tissue repository could not be used to evaluate TRIP13 protein expression in RCC because it showed low or negative immunoreactivity to both recommended antibodies (HPA053093 and HPA005727). Also the group of patients in this trial was small (n = 12).

Role of TRIP13 in cancer

TRIP13 takes part in a variety of cellular activities, including cell cycle regulation, DNA repair and apoptosis. Study on multiple myeloma cells revealed that overexpression of TRIP13 abrogates SAC. The underlying mechanism includes activation of PI3K-Akt signaling pathway that induces proteasome-mediated degradation of MAD2, the key component of SAC [13]. Dysfunctional SAC contributes to chromosomal instability (CIN), aneuploidy, and eventually facilitates cancer progression [14-16]. Moreover, one of major downstream effectors of AKT is the mammalian target of rapamycin (mTOR), which induces cell growth, proliferation, survival, and motility, as well as angiogenesis [17].

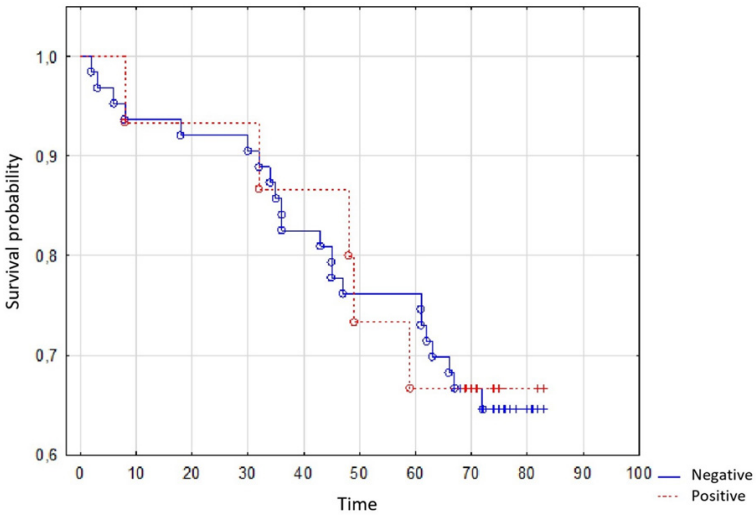

Figure 4. The survival curve of clear cell Renal Cell Carcinoma patients according to TRIP13 nuclear expression.

Table 2. Baseline characteristics of TCGA (n = 528) patient cohort

Clinical information	*n* (%)
Age, yr	
Mean	60.5
Range	26-90
Sex	
Male	344 (65.15)
Female	184 (34.85)
Race	
White	459 (86.93)
Black or African American	54 (10.23)
Asian	8 (1.52)
Unknown	7 (1.33)
Stage	
I	263 (49.81)
II	57 (10.80)
III	123 (23.30)
IV	82 (15.53)
Unknown	3 (0.57)
Median follow up time	3.28
Disease course	
Alive	355 (67.23)
Dead	173 (32.77)

According to study of Yao et al., TRIP13 promotes growth and metastasis of hepatocellular carcinoma through inhibition of TGF-β1/Smad3 signaling [18]. Repressed Smad3 activity has been associated with breast cancer bone metastasis by its effects on tumor angiogenesis, and epithelial-mesenchymal transition (EMT) [19]. Zhou et al. revealed that TRIP13 enhances the proliferation and invasion via activation of the NOTCH signaling and induction of EMT [20]. In damaged cells, TRIP13 functions to favor non-homologous end joining (NHEJ) over homologous recombination (HR). Both are the major pathways for DNA DSBs repair. While HR results in accurate repair, NHEJ is an intrinsically error-prone pathway and may lead to CIN and eventually carcinogenesis [21].

Study of Banerjee et al. demonstrated significant impact of TRIP13 in chemoresistance development among head and neck cancers. Cells with downregulated TRIP13 expression, treated with cisplatin were characterized by better response rate and slower growth [22]. TRIP13 might enhance the resistance to systemic therapy in RCC as well. The systemic therapy (targeted therapy, immunotherapy or chemotherapy) could constitute a selective pressure acting on TRIP13 expression in RCC cells. During the course of the disease, the population of cells with higher expression of TRIP13 would rise because of its protective properties. Ultimately, the cancer tissue would become irreversibly resistant to applied treatment. Our results do not support this hypothesis, because we did not find significant relationships between protein expression and grade or stage of the disease. On the other hand, this approach might be worth pursuing, since the relatively small cohort of advanced ccRCC within our TMA could not ensure a valid representation.

Although the detrimental effect of TRIP13 has been confirmed in biologically diverse neoplasms [13-25], the exact mechanisms and their relative importance are not yet clear. While, as previously described, TRIP13 promotes malignant properties of ovarian cancer cells [20], elevated TRIP13 mRNA expression is associated with favorable outcomes in ovarian

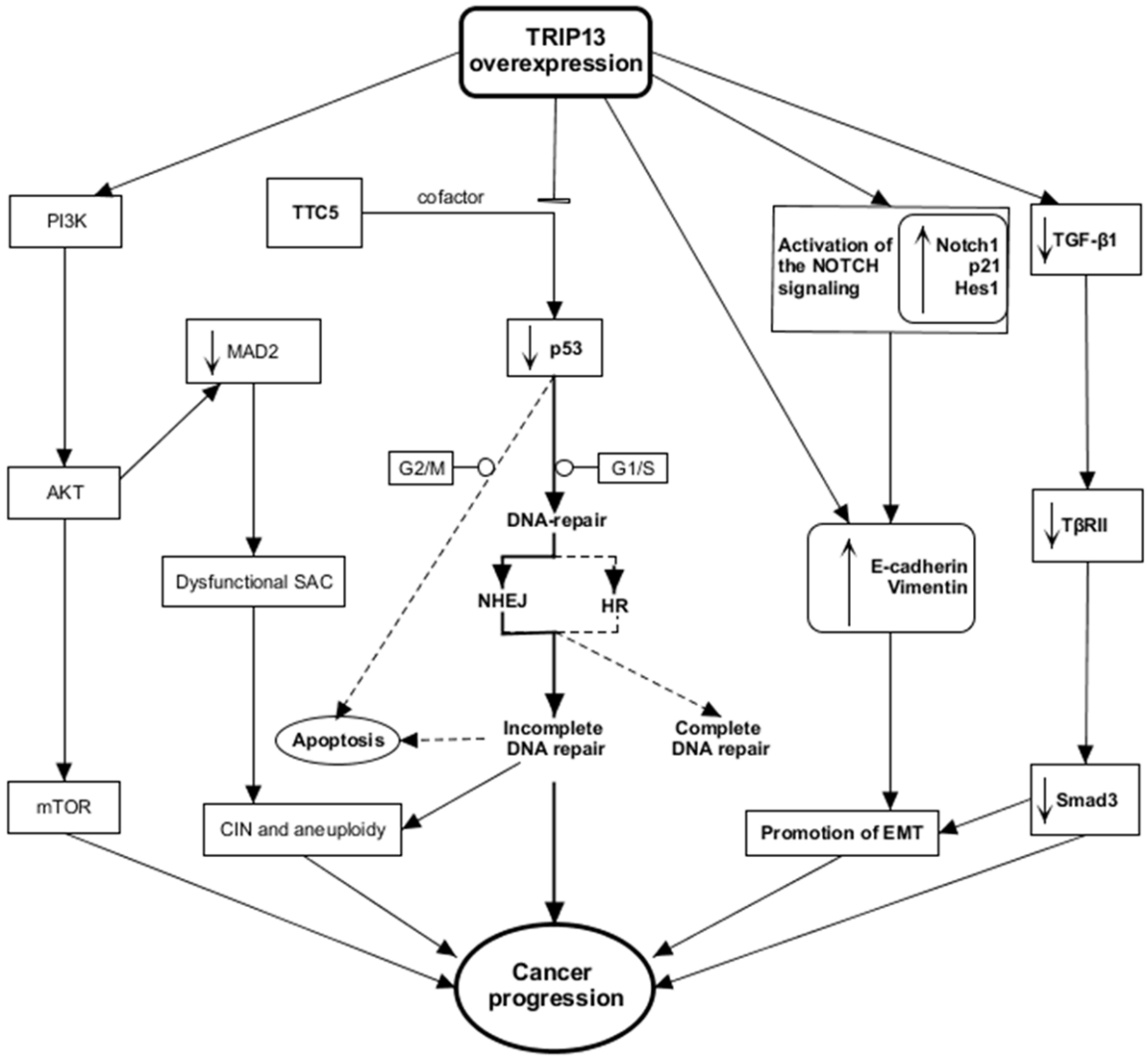

Figure 5. Probable interactions among TRIP13 and other molecules within clear cell Renal Cell Carcinoma. Overexpression of TRIP13 activates PI3K/AKT/mTOR pathway. AKT induces proteasome-mediated degradation of MAD2, the key component of SAC. Dysfunctional SAC leads to CIN and aneuploidy, which, together with mTOR, mediate cancer progression. TRIP13 together with TTC5 as a cofactor, inhibits p53 signaling and, consequently, suppresses the apoptosis. In cells with damaged DNA, TRIP13 functions to favor NHEJ over HR. NHEJ as more likely to be inaccurate, may contribute to cancer progression. TRIP13 also induces the expressions of E-cadherin and vimentin directly or through activation of the NOTCH signaling. The net effect is the promotion EMT, which is directly associated with gain of migratory and invasive capabilities. TRIP13 reduces the expressions of TGF-β1, TβRII and Smad3, the mediators of cellular senescence. The inhibition of TGF-β1/Smad3 signaling supports tumor growth. Decreased Smad3 activity promotes EMT. SAC-spindle assembly checkpoint; CIN-chromosomal instability; NHEJ-non-homologous end joining; HR-homologous recombination; EMT-epithelial-mesenchymal transition.

cancer patients [12]. It demonstrates that the actual contribution of TRIP13 to tumorigenesis could be far more complex.

Role of TRIP13 in kidney

It remains unexplored whether TRIP13 plays a significant role in renal cell carcinoma. However, Pressly et al. recently shed new light on the antiapoptotic role of TRIP13 in renal tubules. As they reported, TRIP13 interacts with Tetratricopeptide Repeat Domain 5 (TTC5) and inhibits p53. Insufficient TRIP13 consequently increases the susceptibility of damaged tubular epithelial cells to progress towards apoptotic cell death [31].

Interestingly, biallelic loss-of-function mutations in TRIP13 have been shown to predispose to Wilms tumor, a kidney cancer that primarily

affects children [32]. The authors of this report indicate a substantial impairment of SAC, which eventually leads to a high rate of chromosome missegregation in these patients. This study supports the existence of a close relationship between TRIP13 and SAC, which when disturbed, increases cancer risk or drives its progression.

Potential role of TRIP13 in renal cell carcinoma

In **Figure 5**, we summarized probable interactions among TRIP13 and other molecules within kidney cancer cell. This pathway diagram illustrates how TRIP13 may affect survival in these patients, and therefore may serve as a starting point for translational research.

It is tempting to speculate, that the ability of TRIP13 to inhibit apoptosis is of paramount importance in RCC patients. Firstly, it has been confirmed in renal tubular epithelial cells, the same that give rise to ccRCC. Secondly, there is accumulating evidence of positive responses to apoptosis inducers in RCC [33-40].

Acknowledgements

This study was supported by grant POWR. 03.02.00-00-I019/16 from The National Centre for Research and Development.

Disclosure of conflict of interest

None.

Address correspondence to: Dr. Adam Kowalewski, Department of Clinical Pathomorphology, Collegium Medicum in Bydgoszcz, Nicolaus Copernicus University in Torun, Poland. Tel: +48-503-134-123; ORCID: 0000-0003-2504-6307; E-mail: kowalewskiresearch@gmail.com

References

[1] American Cancer Society. About Kidney Cancer Overview and Types. 2018.

[2] Choueiri TK and Motzer RJ. Systemic therapy for metastatic renal-cell carcinoma. N Engl J Med 2017; 376: 354-366.

[3] Moch H, Cubilla AL, Humphrey PA, Reuter VE and Ulbright TM. The 2016 WHO classification of tumours of the urinary system and male genital organs-part a: renal, penile, and testicular tumours. Eur Urol 2016; 70: 93-105.

[4] Hsieh JJ, Purdue MP, Signoretti S, Swanton C, Albiges L, Schmidinger M, Heng DY, Larkin J and Ficarra V. Renal cell carcinoma. Nat Rev Dis Prim 2017; 3: 17009.

[5] Gerlinger M, Rowan AJ, Horswell S, Math M, Larkin J, Endesfelder D, Gronroos E, Martinez P, Matthews N, Stewart A, Tarpey P, Varela I, Phillimore B, Begum S, McDonald NQ, Butler A, Jones D, Raine K, Latimer C, Santos CR, Nohadani M, Eklund AC, Spencer-Dene B, Clark G, Pickering L, Stamp G, Gore M, Szallasi Z, Downward J, Futreal PA and Swanton C. Intratumor heterogeneity and branched evolution revealed by multiregion sequencing. N Engl J Med 2012; 366: 883-892.

[6] Stewart GD, O'Mahony FC, Laird A, Eory L, Lubbock ALR, Mackay A, Nanda J, O'Donnell M, Mullen P, McNeill SA, Riddick ACP, Berney D, Bex A, Aitchison M, Overton IM, Harrison DJ and Powles T. Sunitinib treatment exacerbates intratumoral heterogeneity in metastatic renal cancer. Clin Cancer Res 2015; 21: 4212-4223.

[7] Yang WZ, Zhou H and Yan Y. XIAP underlies apoptosis resistance of renal cell carcinoma cells. Mol Med Rep 2017; 17: 125-130.

[8] Rajandram R, Bennett NC, Morais C, Johnson DW and Gobe GC. Renal cell carcinoma: Resistance to therapy, role of apoptosis, and the prognostic and therapeutic target potential of TRAF proteins. Med Hypotheses 2012; 78: 330-336.

[9] Walsh CM. Grand challenges in cell death and survival: apoptosis vs. necroptosis. Front Cell Dev Biol 2014; 2: 3.

[10] Uhlen M, Zhang C, Lee S, Sjöstedt E, Fagerberg L, Bidkhori G, Benfeitas R, Arif M, Liu Z, Edfors F, Sanli K, von Feilitzen K, Oksvold P, Lundberg E, Hober S, Nilsson P, Mattsson J, Schwenk JM, Brunnström H, Glimelius B, Sjöblom T, Edqvist PH, Djureinovic D, Micke P, Lindskog C, Mardinoglu A and Ponten F. A pathology atlas of the human cancer transcriptome. Science 2017; 357: eaan2507.

[11] Budczies J, Klauschen F, Sinn B V, Győrffy B, Schmitt WD, Darb-Esfahani S and Denkert C. Cutoff Finder: a comprehensive and straightforward Web application enabling rapid biomarker cutoff optimization. PLoS One 2012; 7: e51862.

[12] KIDNEY RENAL CLEAR CELL CARCINOMA (KIRC)-Interactive survival scatter plot & Survival analysis, TCGA RNA samples/data available from v18.1.proteinatlas.org. no date.

[13] Tao Y, Yang G, Yang H, Song D, Hu L, Xie B, Wang H, Gao L, Gao M, Xu H, Xu Z, Wu X, Zhang Y, Zhu W, Zhan F and Shi J. TRIP13 impairs mitotic checkpoint surveillance and is associated with poor prognosis in multiple myeloma. Oncotarget 2017; 8: 26718-26731.

[14] Ma HT and Poon RYC. TRIP13 regulates both the activation and inactivation of the spindle-assembly checkpoint. Cell Rep 2016; 14: 1086-1099.
[15] Kops GJPL, Weaver BAA and Cleveland DW. On the road to cancer: aneuploidy and the mitotic checkpoint. Nat Rev Cancer 2005; 5: 773-85.
[16] Fang X and Zhang P. Aneuploidy and tumorigenesis. Semin Cell Dev Biol 2011; 22: 595-601.
[17] Laplante M and Sabatini DM. mTOR signaling in growth control and disease. Cell 2012; 149: 274-93.
[18] Yao J, Zhang X, Li J, Zhao D, Gao B, Zhou H, Gao S and Zhang L. Silencing TRIP13 inhibits cell growth and metastasis of hepatocellular carcinoma by activating of TGF-β1/smad3. Cancer Cell Int 2018; 18: 208.
[19] Petersen M, Pardali E, van der Horst G, Cheung H, van den Hoogen C, van der Pluijm G and Ten Dijke P. Smad2 and Smad3 have opposing roles in breast cancer bone metastasis by differentially affecting tumor angiogenesis. Oncogene 2010; 29: 1351-61.
[20] Zhou XY and Shu XM. TRIP13 promotes proliferation and invasion of epithelial ovarian cancer cells through Notch signaling pathway. Eur Rev Med Pharmacol Sci 2019; 23: 522-529.
[21] Sheng N, Yan L, Wu K, You W, Gong J, Hu L, Tan G, Chen H and Wang Z. TRIP13 promotes tumor growth and is associated with poor prognosis in colorectal cancer. Cell Death Dis 2018; 9: 402.
[22] Banerjee R, Russo N, Liu M, Basrur V, Bellile E, Palanisamy N, Scanlon CS, van Tubergen E, Inglehart RC, Metwally T, Mani RS, Yocum A, Nyati MK, Castilho RM, Varambally S, Chinnaiyan AM and D'Silva NJ. TRIP13 promotes error-prone nonhomologous end joining and induces chemoresistance in head and neck cancer. Nat Commun 2014; 5: 4527.
[23] Cao Y, Zhu W, Chen W, Wu J, Hou G and Li Y. Prognostic value of BIRC5 in lung adenocarcinoma lacking EGFR, KRAS, and ALK mutations by integrated bioinformatics analysis. Dis Markers 2019; 2019: 1-12.
[24] Di S, Li M, Ma Z, Guo K, Li X and Yan X. TRIP13 upregulation is correlated with poor prognosis and tumor progression in esophageal squamous cell carcinoma. Pathol Res Pract 2019; 152415.
[25] Yan X, Guo Z, Liu X, Feng Y, Zhao Y, Liu T and Li S. Four novel biomarkers for bladder cancer identified by weighted gene coexpression network analysis. J Cell Physiol 2019; 234: 19073-19087.
[26] Zhang X, Zhou J, Xue D, Li Z, Liu Y and Dong L. MiR-515-5p acts as a tumor suppressor via targeting TRIP13 in prostate cancer. Int J Biol Macromol 2019; 129: 227-232.
[27] Liu M, Qiu Y, Jin T, Zhou Y, Mao Z and Zhang Y. Meta-analysis of microarray datasets identify several chromosome segregation-related cancer/testis genes potentially contributing to anaplastic thyroid carcinoma. PeerJ 2018; 6: e5822.
[28] Phan NN, Wang CY, Li KL, Chen CF, Chiao CC, Yu HG, Huang PL and Lin YC. Distinct expression of CDCA3, CDCA5, and CDCA8 leads to shorter relapse free survival in breast cancer patient. Oncotarget 2018; 9: 6977-6992.
[29] Zhou K, Zhang W, Zhang Q, Gui R, Zhao H, Chai X, Li Y, Wei X and Song Y. Loss of thyroid hormone receptor interactor 13 inhibits cell proliferation and survival in human chronic lymphocytic leukemia. Oncotarget 2017; 8: 25469-25481.
[30] Dazhi W, Mengxi Z, Fufeng C and Meixing Y. Elevated expression of thyroid hormone receptor-interacting protein 13 drives tumorigenesis and affects clinical outcome. Biomark Med 2017; 11: 19-31.
[31] Pressly JD, Hama T, Brien SO, Regner KR and Park F. TRIP13-deficient tubular epithelial cells are susceptible to apoptosis following acute kidney injury. Sci Rep 2017; 7: 43196.
[32] Yost S, Wolf B de, Hanks S, Zachariou A, Marcozzi C, Clarke M, Voer R de, Etemad B, Uijttewaal E, Ramsay E, Wylie H, Elliott A, Picton S, Smith A, Smithson S, Seal S, Ruark E, Houge G, Pines J, Kops GJPL and Rahman N. Biallelic TRIP13 mutations predispose to Wilms tumor and chromosome missegregation. Nat Genet 2017; 49: 1148-1151.
[33] Frees S, Chavez-Munoz C, Zhou B, Raven P, Fazli L, Chi K, Lawson K, Finelli A, Gleave M and So A. Targeting heat-shock protein 27 enhances sensitivity to sorafenib treatment in renal cancer in vitro and in vivo. Eur Urol Suppl 2017; 16: e1480.
[34] Aggarwal R, Thomas S, Pawlowska N, Bartelink I, Grabowsky J, Jahan T, Cripps A, Harb A, Leng J, Reinert A, Mastroserio I, Truong TG, Ryan CJ and Munster PN. Inhibiting histone deacetylase as a means to reverse resistance to angiogenesis inhibitors: phase I study of abexinostat plus pazopanib in advanced solid tumor malignancies. J Clin Oncol 2017; 35: 1231-1239.
[35] Pili R, Quinn DI, Hammers HJ, Monk P, George S, Dorff TB, Olencki T, Shen L, Orillion A, Lamonica D, Fragomeni RS, Szabo Z, Hutson A, Groman A, Perkins SM, Piekarz R and Carducci MA. Immunomodulation by entinostat in renal cell carcinoma patients receiving high-dose interleukin 2: a multicenter, single-arm, phase I/II Trial (NCI-CTEP#7870). Clin Cancer Res 2017; 23: 7199-7208.
[36] Sato H, Uzu M, Kashiba T, Suzuki R, Fujiwara T, Okuzawa H and Ueno K. Sodium butyrate enhances the growth inhibitory effect of sunitinib

in human renal cell carcinoma cells. Oncol Lett 2017; 14: 937-943.
[37] Pili R, Liu G, Chintala S, Verheul H, Rehman S, Attwood K, Lodge MA, Wahl R, Martin JI, Miles KM, Paesante S, Adelaiye R, Godoy A, King S, Zwiebel J and Carducci MA. Combination of the histone deacetylase inhibitor vorinostat with bevacizumab in patients with clear-cell renal cell carcinoma: a multicentre, single-arm phase I/II clinical trial. Br J Cancer 2017; 116: 874-883.
[38] Mao S, Lu G, Lan X, Yuan C, Jiang W, Chen Y, Jin X and Xia Q. Valproic acid inhibits epithelial-mesenchymal transition in renal cell carcinoma by decreasing SMAD4 expression. Mol Med Rep 2017; 16: 6190-6199.
[39] Wei M, Mao S, Lu G, Li L, Lan X, Huang Z, Chen Y, Zhao M, Zhao Y and Xia Q. Valproic acid sensitizes metformin-resistant human renal cell carcinoma cells by upregulating H3 acetylation and EMT reversal. BMC Cancer 2018; 18: 434.
[40] Nitta T, Koike H, Miyao T, Miyazawa Y, Kato H, Furuya Y, Sekine Y and Suzuki K. YM155 reverses statin resistance in renal cancer by reducing expression of survivin. Anticancer Res 2017; 37: 75-80.